

## Specific-heat measurements of $\text{Ho}_x\text{Y}_{1-x}\text{Co}_2$

G. Hilscher, N. Pillmayr, C. Schmitzer, and E. Gratz

*Institute of Experimental Physics, Technical University of Vienna, Karlsplatz 13, A-1040 Vienna, Austria*

(Received 8 June 1987)

We report on specific-heat measurements of  $(\text{Ho}_x\text{Y}_{1-x})\text{Co}_2$  in the temperature range from 1.5 to 60 K. Sharp peaks at the Curie temperature  $T_C$  and the spin-reorientation temperature  $T_r$  characterize the temperature dependence for  $0.5 \leq x \leq 1$ . For  $0.2 \leq x \leq 0.4$  the magnetic specific heat  $C_m$  indicates spin-glass-like behavior, which appears to be in agreement with freezing phenomena observed in magnetic measurements. From the analysis of the magnetic entropy  $S_m$ , we deduce that the induced Co moment can be referred to as itinerant in the sense of the Stoner theory. In the dilute Ho-concentration range, various anomalies are observed as, e.g., an enhancement of the effective electronic specific heat  $\gamma$  and the effective Debye temperature  $\Theta_D$  (of about 400% and 100%, respectively) and significant upturns of the  $C_p/T$  versus  $T^2$  graphs together with a pronounced reduction of the magnetic entropy. These anomalies are discussed in terms of spin fluctuations; the loss of the magnetic entropy for  $x < 0.2$  may point to an instability of the Ho moment.

### I. INTRODUCTION

The cubic Laves-phase compounds  $R\text{Co}_2$  ( $R$ =a rare-earth element) attracted growing interest because of the particular magnetic properties which are correlated with the onset of itinerant-electron magnetism of the Co 3d electrons induced by the local 4f moments.<sup>1-3</sup> If the rare-earth element carries no moment in  $R\text{Co}_2$  we have to deal with compounds as  $\text{YCo}_2$  and  $\text{LuCo}_2$  which are on the border to magnetism and are well known for their exchange-enhanced properties<sup>4,5</sup> and the occurrence of spin fluctuations.<sup>6</sup> In particular,  $\text{YCo}_2$  was supposed to be an itinerant metamagnet,<sup>7-10</sup> where the critical field of the metamagnetic transition was recently predicted from several band-structure calculations ranging from 90 to 350 T.

In the heavy rare-earth compounds  $R\text{Co}_2$  a Co moment of about  $1\mu_B$  is induced by the 4f molecular field.<sup>11,3</sup> The transition from ferrimagnetism to paramagnetism is of first order for  $\text{DyCo}_2$ ,  $\text{HoCo}_2$ , and  $\text{ErCo}_2$  but of second order for  $\text{GdCo}_2$  and  $\text{TbCo}_2$ . Bloch *et al.*<sup>12</sup> discussed the first- and second-order phase transitions in terms of the Landau theory. They suggested that the order of the phase transition depends upon a change of the sign of the Landau parameter  $B(T)$  which appears in the free-energy expansion in powers of the magnetization.  $B(T)$  is the second term of this expansion and its sign is intimately associated with the susceptibility of the itinerant 3d electrons. Recently Duc *et al.*<sup>13</sup> confirmed this hypothesis with new experimental data on  $(\text{Er},\text{Y})\text{Co}_2$  which they analyzed with a further developed type of the above-mentioned model<sup>14</sup> also including the contribution of the rare-earth magnetization.

Therefore, pseudobinary systems as  $(R,\text{Y})\text{Co}_2$  where the local 4f moment is diluted by Y are considered to be good candidates to study the onset of the induced itinerant-electron (Co 3d) magnetism. Around this concentration, where the induced moment occurs, freezing

phenomena in the magnetization<sup>3</sup> and appreciable anomalies of the transport properties in the form of significant minima in resistivity and thermopower have been observed recently.<sup>15</sup> However, most of the numerous previous investigations<sup>3,16-19</sup> have been centered on the question "in which respect is the Co moment induced, what is its extent of itinerancy and at which internal molecular field does this occur." This is of relevance for the critical fields of the metamagnetic transition in  $\text{YCo}_2$  predicted by band-structure calculations since these are beyond the laboratory scale. Thermal-expansion experiments confirmed the induced itinerant character of the Co moment.<sup>3,18,13</sup>

Our initial object of the present work was to perform specific-heat measurements on these pseudobinaries in order to resolve the large anomalies in the resistivity and thermopower which seem to be associated with the onset of 3d magnetism. This was recently discussed in terms of spin fluctuations and/or a possible Kondo scattering mechanism.<sup>15</sup>

### II. EXPERIMENTAL PROCEDURE

The samples were prepared by high-frequency melting of 99.99%-pure Ho, Y, and Co under an argon protective atmosphere. To avoid the appearance of foreign phases a 6-wt. % excess of R over the nominal stoichiometric composition was used. After annealing under vacuum at 900°C for 1 week the samples were checked for phase purity by Debye-Scherrer photographs.

The specific-heat measurements were performed in an automated adiabatic calorimeter in the temperature range 1.5–60 K.<sup>20</sup> The calorimeter was calibrated and tested using high-purity (99.999%) copper with the result that the absolute accuracy is estimated to be better than 1% in the low-temperature range and  $\pm 3\%$  for  $T > 30$  K.

### III. RESULTS

The magnetic phase diagram with the ferromagnetic Curie temperatures  $T_C$ , the freezing temperatures  $T_f$ , and the spin-reorientation temperatures  $T_r$  is shown (Fig. 1).  $T_C$ ,  $T_f$ , and  $T_r$  were determined by magnetization, dc, and ac susceptibility measurements. At  $T_r$  the easy axis of magnetization changes from [100] to [110].<sup>21,22</sup> For  $x \leq 0.4$  freezing phenomena are already observed in the magnetization, measured with and without field cooling. These observations are in agreement with previous magnetization measurements by Steiner *et al.*<sup>3</sup> The ac susceptibility curves exhibit sharp cusps not only at the transition temperatures  $T_C$  and  $T_r$  in the long-range-ordered regime ( $x > 0.4$ ) but also at the freezing temperatures  $T_f$  for  $x \leq 0.4$ . From a discontinuous change of the magnetization and the resistivity at  $T_C$  together with thermal hysteresis effects it was concluded<sup>15</sup> that the transition at  $T_C$  is of first order for  $x \geq 0.6$ , whereas for  $x = 0.5$  a second-order phase transition occurs. Reducing further the Ho concentration no long-range order can be detected from Arrott plots (for  $x \leq 0.4$ ) but freezing effects occur in the magnetization on cooling the sample with and without field.

The concentration-dependent change of the type of the magnetic transition from first to second order and further to disorder can nicely be observed in specific-heat measurements shown in Fig. 2. For  $x = 0.6$  the peak at  $T_C$  is very sharp and symmetric indicating a first-order transition; the rounded peak at  $T_C$  for  $x = 0.5$  points to a second-order phase transition, but the spin reorientation is still present. No transition to a long-range magnetic order can be deduced from the broad maximum of the specific heat for  $x = 0.4$  which also points to a random freezing of magnetic moments.

These freezing phenomena seem to be dominant for  $x \leq 0.4$  and give rise to a large magnetic contribution to

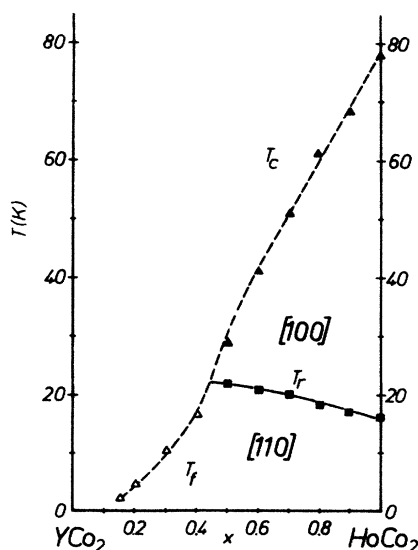


FIG. 1. Magnetic phase diagram of  $(\text{Ho}_x\text{Y}_{1-x})\text{Co}_2$  ( $\blacktriangle$ : Curie temperature  $T_C$ ;  $\triangle$ : spin-freezing temperature  $T_f$ ;  $\blacksquare$ : spin-reorientation temperature  $T_r$ ).

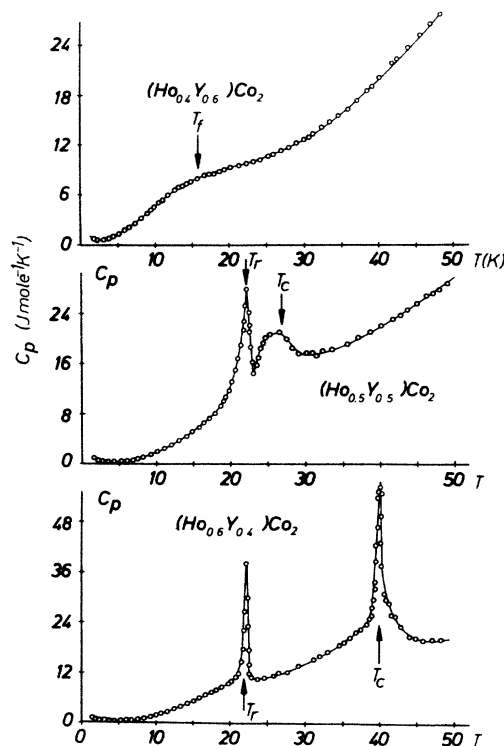


FIG. 2. The temperature dependence of the specific-heat  $C_p$  of  $(\text{Ho}_x\text{Y}_{1-x})\text{Co}_2$  for  $0.4 \leq x \leq 0.6$  (arrows indicate  $T_C$ ,  $T_f$ , and  $T_r$ ).

the specific heat. Apart from the anomalies at  $T_C$ ,  $T_r$ , and  $T_f$  we observe a large nuclear specific heat due to the hyperfine splitting of the  $I = \frac{7}{2}$  Ho nucleus at low temperatures besides the nonmagnetic electron ( $C_e$ ) and phonon contribution ( $C_{ph}$ ) to the heat capacity.

To analyze the specific heat we use the following expression:

$$C_p = \gamma T + \beta T^3 + C_n + C_m \quad (1)$$

with the electronic ( $\gamma$ ) and the lattice ( $\beta$ ) specific-heat coefficients, which are related to the density of states  $N(E_f)$  and the Debye temperature  $\Theta_D$ , respectively. A nuclear contribution to the specific-heat  $C_n$  arises when the  $(2I + 1)$ -fold degeneracy of the nuclear state is removed by the hyperfine field and/or the quadrupole moment giving rise to a Schottky-type specific-heat anomaly associated with the eigenvalues<sup>23</sup>

$$E_m / k_B = a' m + P \left[ m^2 - \frac{1}{3} I(I + 1) \right] \quad (2)$$

$m = 0, 1, \dots, 2I + 1$

The parameters  $a'$  and  $P$  are related to the hyperfine field  $H_{\text{eff}}$  and the quadrupole moment  $eQ$ :

$$a' = (\mu_I H_{\text{eff}}) / (k_B I), \quad (3a)$$

$$P = (3e^2 q Q) / [4k_B I(2I - 1)]. \quad (3b)$$

The magnetic contribution to the heat capacity  $C_m$  can have different origins, in particular, for the long-range-ordered and the spin-glass range. Therefore we subdivide

the analysis of  $C_m$  of  $(\text{Ho}_x\text{Y}_{1-x})\text{Co}_2$  into the long-range-ordered regime ( $0.5 \leq x \leq 1.0$ ) and the magnetically disordered concentration range.

#### A. $0.5 \leq x \leq 1.0$

Castets, Gignoux, and Hennion<sup>24</sup> deduced from inelastic neutron scattering on a  $\text{HoCo}_2$  single crystal that the magnetic excitations follow the spin-wave dispersion relation  $\omega_q = \omega_0 + Dq^2$  with  $\omega_0 = 6.1$  THz and  $D = 62$  THz  $\text{\AA}^2$ . The gap observed for a vanishing reduced wave vector  $q$  arises from the action of the Ho molecular field upon the Co ions and corresponds to a temperature  $T_0$  of 46.6 K.  $C_m$  related to this spin-wave dispersion relation is given by

$$C_m = BT^{3/2} \exp(-T_0/T) \quad (4)$$

with  $B = \frac{15}{4} k_B V [k_B / (2Dh)]^{3/2}$  according to Keffer.<sup>25</sup> The spin-wave-stiffness constant deduced from neutron diffraction gives  $B = 4.3 \text{ mJ K}^{-5/2} \text{ mole}^{-1}$  for  $\text{HoCo}_2$  with a molar volume  $V$  of  $38 \text{ cm}^3 \text{ mole}^{-1}$ . In order to search for the spin-wave contribution we analyzed the heat capacity for  $x \geq 0.5$  from 1.5 to 10 K with the following expression:

$$C_p - C_n = \gamma T + \beta T^3 + BT^{3/2} \exp(-T_0/T) \quad (5)$$

using a standard least-squares routine (NAGLIB, E04KCF). The result of this procedure is an almost constant nuclear specific heat per Ho atom for the concentration range under consideration and a slight variation of  $\gamma$  and  $\beta$  which are given in Table I. However, we were not successful in determining the spin-wave contribution  $BT^{3/2} \exp(-T_0/T)$ . This contribution is very small compared to the grand total heat capacity (of the order of 1% at 10 K, about  $1 \text{ mJ mole}^{-1} \text{ K}^{-1}$ ) because of the large gap  $T_0$

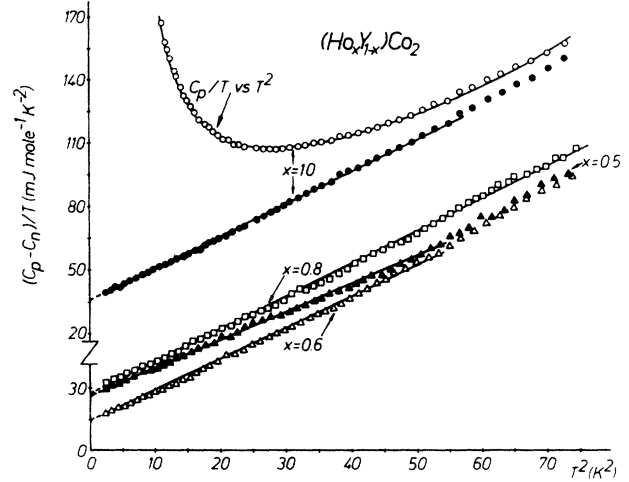


FIG. 3.  $(C_p - C_n)/T$ -vs- $T^2$  graphs of  $(\text{Ho}_x\text{Y}_{1-x})\text{Co}_2$  for  $0.6 \leq x \leq 1$ ; the  $C_p/T$ -vs- $T^2$  graph of  $\text{HoCo}_2$  is shown for comparison.

and a comparatively small coefficient  $B$ . This is also demonstrated in Fig. 3 where  $C_p/T$  of  $\text{HoCo}_2$  and  $(C_p - C_n)/T$  of  $(\text{Ho}_x\text{Y}_{1-x})\text{Co}_2$  ( $x = 1.0, 0.8, 0.6$ , and  $0.5$ ) is plotted against  $T^2$ .  $(C_p - C_n)/T$  plots appear to be fairly linear, indicating no significant extra contribution to  $C_p$ .

#### B. $0.0 < x < 0.5$

In order to separate the various contributions to  $C_p$  in this composition range it was necessary to assume that the hyperfine field on the Ho nucleus, giving rise to the large  $C_n$ , remains almost constant in the spin-glass range and even in the dilute concentration range below  $x = 0.1$ .

TABLE I.  $\gamma, \beta, T_c, T_r, T_f$ , and  $T^* = T(C_{m,\max})$  for  $(\text{Ho}_x\text{Y}_{1-x})\text{Co}_2$ .

$x$	$\gamma$ (mJ mole <sup>-1</sup> K <sup>-2</sup> )	$\beta$ (mJ mole <sup>-1</sup> K <sup>-4</sup> )	$T_c$ (K)	$T_r$ (K)	$T_f$ (K)	$T^*$ (K)
0.000	36.5	0.500				11.0
0.020	46.0	0.274				10.2
0.040	62.5	0.249				10.2
0.050	60.0	0.232				10.2
0.060	65.0	0.216				10.2
0.100	90.0	0.199				10.1
0.125	101.0	0.186				8.5
0.150	120.0	0.168			2.2	8.1
0.175	136.0	0.159				8.0
0.200	160.0	0.161			4.6	9.1
0.300	136.0				10.5	12.4
0.400	71.0				16.5	16.9
0.500	28.0	1.451	27	22.0		
0.600	13.0	1.507	40	22.0		
0.700			51	20.0		
0.800	25.5	1.322	61	18.5		
0.900			68	17.0		
1.000	37.0	1.507	78	16.0		

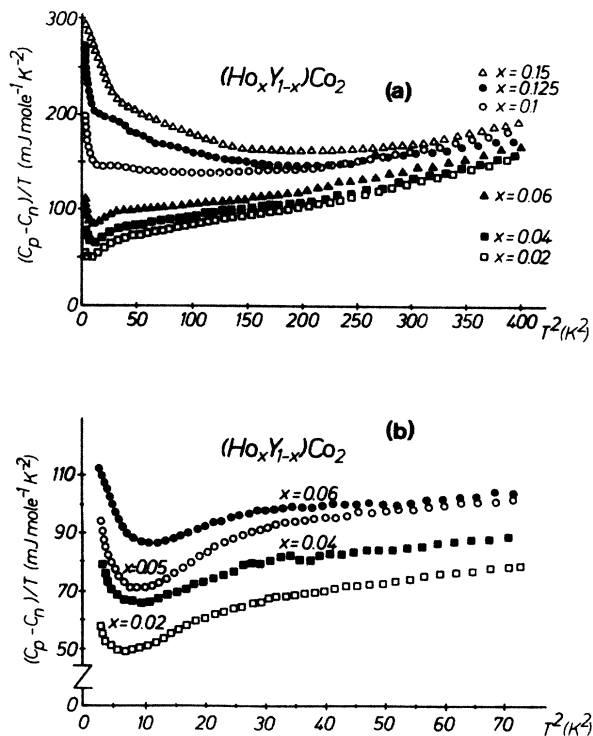


FIG. 4. (a) and (b).  $(C_p - C_n)/T$ -vs- $T^2$  graphs of  $(\text{Ho}_x\text{Y}_{1-x})\text{Co}_2$  for  $0 < x \leq 0.15$ .

This is reasonable for the spin-glass range, since it is well known that the hyperfine field attains almost the full value of the ordered compounds in this state<sup>26,27</sup> and breaks down only in the very dilute concentration range. Therefore the above assumption appears to be rather questionable for  $x < 0.1$ . Thus we tried to determine  $C_n$  from the low-temperature upturn using a least-squares routine, but the hyperfine parameters obtained turned out to be unreasonably high, particularly in the dilute range ( $x < 0.125$ ). However, appreciably low temperature upturns are observed in the  $(C_p - C_n)/T$ -versus- $T^2$  plots, presented in Figs. 4(a) and 4(b), although the full  $C_n$  per Ho atom is used even in the dilute limit. Therefore upturns are supposed to arise from other mechanisms (such as, e.g., spin fluctuations and/or Kondo scattering, to which we come back later) since in any case we subtract a larger nuclear contribution rather than one that is too small.

In spite of the enormous magnetic heat capacity (Fig. 5)  $\gamma$  and  $\beta$  could be derived reasonably accurately for  $0.0 < x < 0.2$  from the fairly linear high-temperature part of  $(C_p - C_n)/T$ -versus- $T^2$  plots shown in Fig. 6. For the compounds with  $x = 0.3$  and  $0.4$ , which are on the border for the onset of long-range order, the large magnetic hump extends up to high temperatures (40 K). To determine  $\gamma$  and  $\beta$  for both compounds we therefore used, instead of the high-temperature part, the low-temperature part of the  $(C_p - C_n)/T$ -versus- $T^2$  plot, where the  $C_m$  can be assumed to be drastically reduced. The  $\gamma$  and  $\beta$  values derived by these procedures are listed together in Table I with the ordering temperatures  $T_C$ , the spin-

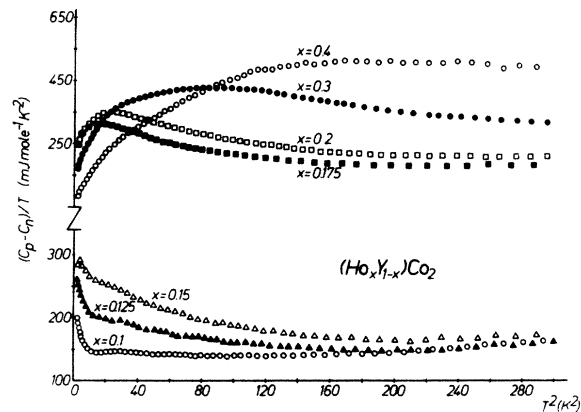


FIG. 5.  $(C_p - C_n)/T$ -vs- $T^2$  graphs of  $(\text{Ho}_x\text{Y}_{1-x})\text{Co}_2$  for  $0.1 \leq x \leq 0.4$ .

reorientation temperatures  $T_r$ , the freezing temperatures  $T_f$ , and the position of the maxima of  $C_m$ :  $T^* = T(C_{m,\max})$ . The variation of the effective  $\gamma$  value and the effective Debye temperature  $\Theta_D$  with the Ho content is graphically presented in Fig. 7. We suppose that the enhancement of  $\gamma$  and  $\Theta_D$  is predominantly of magnetic origin (as spin fluctuations and/or presumably the Kondo scattering mechanism).

To obtain the magnetic heat capacity we subtract both the nuclear and the nonmagnetic heat capacity, whereby the latter is approximated by the specific heat of the exchange-enhanced Pauli paramagnet  $\text{YCo}_2$ . This is reasonable for  $0.0 < x < 0.125$  since the  $(C_p - C_n)/T$ -versus- $T^2$  graphs of those compounds closely approach that of  $\text{YCo}_2$  at high temperatures. Only for  $x = 0.2, 0.3$ , and  $0.4$  are these plots shifted to higher  $C_p/T$  values at higher temperatures, which is, compared with the large magnetic hump, presumably of minor importance for the determination of  $C_m$  (Fig. 6).

Considering the freezing phenomena in the magnetization we found that the magnetic heat capacity—obtained as described above—displays broad anomalies with maxi-

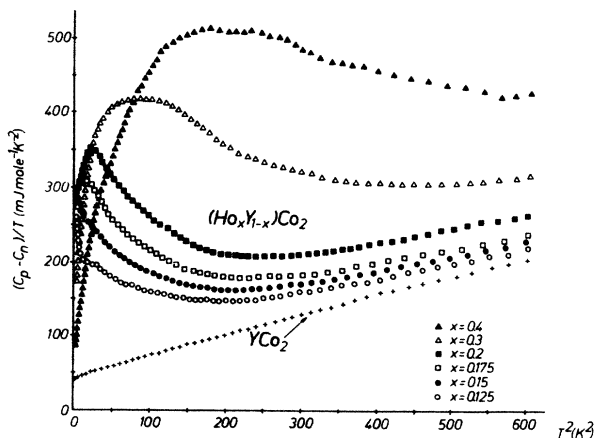


FIG. 6.  $(C_p - C_n)/T$ -vs- $T^2$  graphs of  $(\text{Ho}_x\text{Y}_{1-x})\text{Co}_2$  and for  $\text{YCo}_2$ ,  $0.125 \leq x \leq 0.4$ .

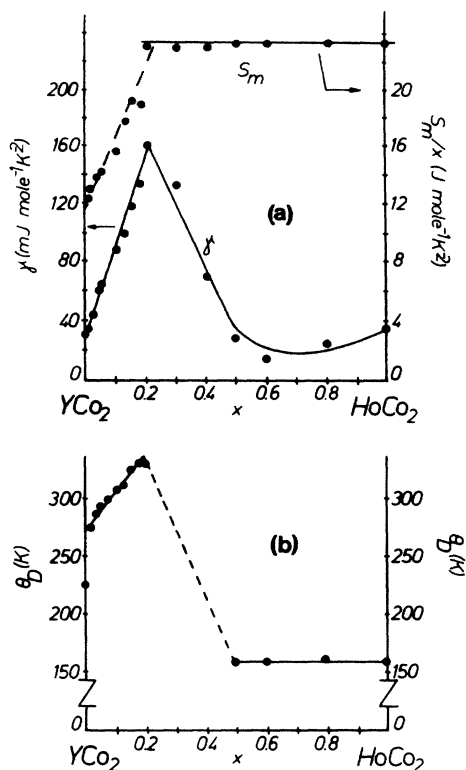


FIG. 7. (a) Concentration dependence of the effective electronic specific-heat  $\gamma$  (i.e., the contribution to the heat-capacity linear in  $T$ ) and the magnetic entropy per Ho atom  $S_m/x$  of  $(\text{Ho}_x\text{Y}_{1-x})\text{Co}_2$  for  $0 \leq x \leq 1$ . (b) Variation of the effective Debye temperature  $\Theta_D$  as a function of  $x$  for  $(\text{Ho}_x\text{Y}_{1-x})\text{Co}_2$ .

ma above the sharp susceptibility cusps, indicating also that the magnetic moments are frozen in random directions.

Souletie and Tournier<sup>28</sup> derived for dilute magnetic alloy systems that the thermodynamic properties can be expressed in terms of a universal function of the reduced temperature  $T/x$  with  $x$  the concentration. This result is based on the assumption that the magnetic interaction in dilute alloys (as, e.g.,  $\text{CuMn}$ ,  $\text{AuFe}$ ) proceeds via the Ruderman-Kittel-Kasuya-Yosida (RKKY) interaction which is proportional to  $1/r^3$ ;  $r$  is the distance between the magnetic ions. With the use of the relation  $xr^3=1$ , they deduced that for sufficiently low temperatures and concentrations  $C_m/x$  scales with  $T/x$ . Figure 8(a) demonstrates that  $C_m/x$  scales approximately with  $T/x$ ; however, a better scaling is obtained for  $0.15 < x \leq 0.4$  if we use  $C_m/x^{1.7}$  instead of  $C_m/x$  [Fig. 8(b)].

Although the model was originally proposed for dilute alloys, the present results indicate that a random freezing of the Ho moments occur in the concentrated composition range despite of these deviations from the idealized simple model. Nevertheless, this model also provides a reasonably accurate description of this type of concentrated alloy since the magnetic interaction for rare-earth metals always proceeds via the RKKY exchange, but can obviously be applied for magnetic 3d impurities in the dilute limit only.

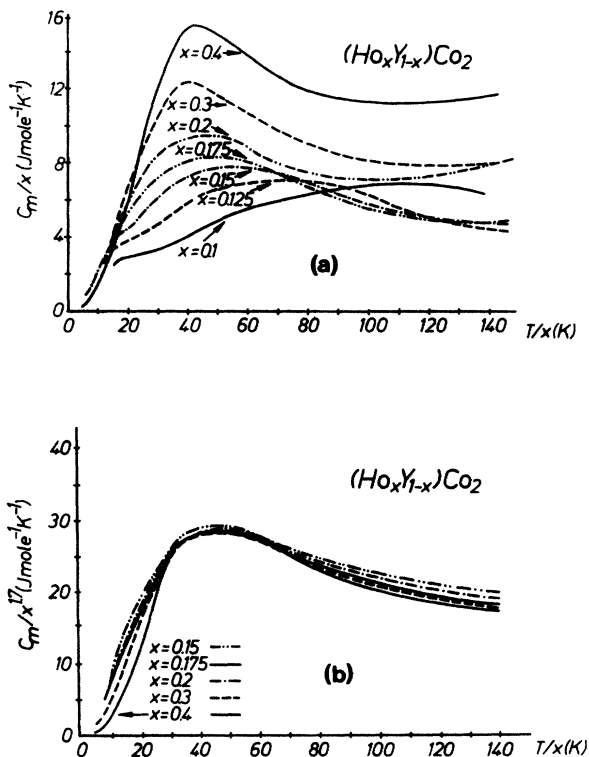


FIG. 8. (a) The reduced magnetic contribution to the heat capacity  $C_m/x$  vs the reduced temperature  $T/x$  of  $(\text{Ho}_x\text{Y}_{1-x})\text{Co}_2$  for  $0.1 \leq x \leq 0.4$ . (b)  $C_m/x^{1.7}$  vs  $T/x$  of  $(\text{Ho}_x\text{Y}_{1-x})\text{Co}_2$  for  $0.15 \leq x \leq 0.4$ .

Below  $x=0.175$  the system behaves distinctly differently: The maxima of  $C_m$  remain almost constant at about 10 K while the cusps of the ac susceptibility decrease steadily upon lowering the Ho content and  $C_m/x$  appears to follow a universal function of  $T$  (Fig. 9). This is probably correlated with the onset of an induced itinerant Co moment at about this Ho concentration.

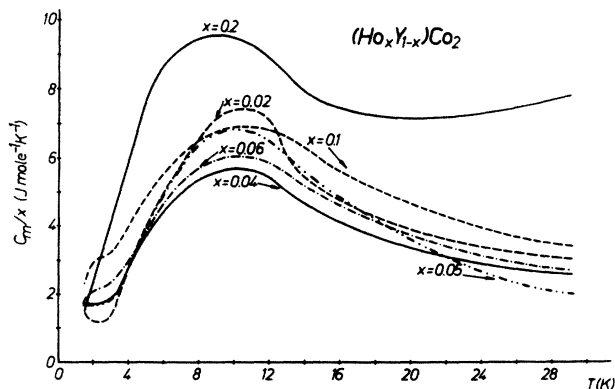


FIG. 9.  $C_m/x$  vs  $T$  of  $(\text{Ho}_x\text{Y}_{1-x})\text{Co}_2$  for  $0 < x \leq 0.2$ .

## IV. DISCUSSION

One of the most remarkable features of the magnetic phase diagram of these compounds is that more than 40% Ho (substitution) is necessary to establish long-range magnetic order. This is noteworthy since it is well known that the exchange-enhanced Pauli paramagnet  $\text{YCo}_2$  is on the verge of magnetism as mentioned in Sec. I.

Schwarz and Mohn<sup>9</sup> demonstrated that the critical field of the metamagnetic transition in  $\text{YCo}_2$  sensitively depends on the volume: A slight volume expansion was already supposed to reduce the critical field into a range attainable in the laboratory. The appearance of magnetism in  $\text{Y}(\text{Co}_{1-x}\text{Al}_x)_2$  can be used as experimental evidence for the above-mentioned predictions, since the substitution of Co by Al causes the lattice expansion required to stabilize magnetism via foregoing metamagnetism.<sup>29</sup>

A comparison with other heavy  $(R, \text{Y})\text{Co}_2$  systems ( $R = \text{Gd}-\text{Tm}$ ) shows that the critical concentration  $x_c$  for the onset of magnetism depends on the magnetic exchange energy of the boundary compounds  $R\text{Co}_2$ .  $x_c$  becomes larger in these pseudobinaries as one proceeds in this series from Gd to Tm since  $T_C$  and  $\Theta_p$  decrease linearly with the de Gennes factor (see Fig. 10): In a first approximation we found that  $x_c$  of these pseudobinaries varies inversely with  $T_C$  and the de Gennes factor of the respective  $R\text{Co}_2$  compounds. Additionally we suppose from recent specific-heat measurements of  $(\text{Dy}, \text{Y})\text{Co}_2$  (Ref. 30),  $(\text{Tb}, \text{Y})\text{Co}_2$  (Ref. 31), and  $(\text{Er}, \text{Y})\text{Co}_2$  (Ref. 32) that the maximum of the enhanced  $\gamma$  value varies as  $x_c$  inversely with the de Gennes factor (at about or just below the critical concentration). The maximal  $\gamma$  factor of  $(\text{Tb}, \text{Y})\text{Co}_2$  is  $69 \text{ mJ mole}^{-1} \text{K}^{-2}$  (Ref. 31) and that of

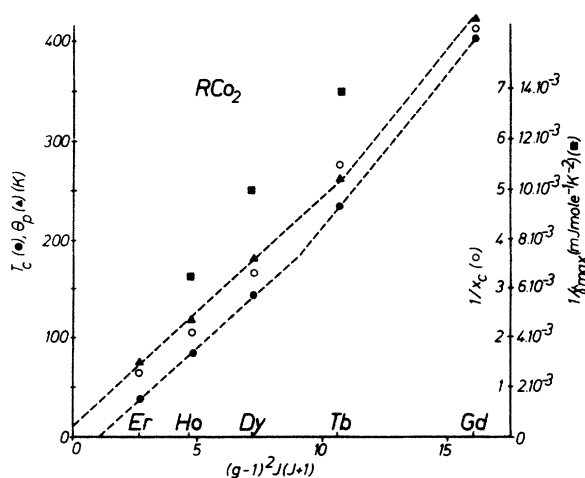


FIG. 10. The ferromagnetic [ $T_C$  (●)] and paramagnetic Curie temperatures [ $\Theta_p$  (▲)] as a function of the de Gennes factor  $(g-1)^2 J(J+1)$  for  $R\text{Co}_2$  ( $R = \text{Er}, \text{Ho}, \text{Dy}, \text{Tb}, \text{Gd}$ );  $T_C$  and  $\Theta_p$  values according to Buschow (Ref. 33). The reciprocal maximal  $\gamma$  value  $1/\gamma$  (■) and the reciprocal critical concentration  $1/x_c$  (○) for the onset of long-range order of the pseudobinaries  $(R_x\text{Y}_{1-x})\text{Co}_2$  as a function of the de Gennes factor.

the Ho system reaches  $160 \text{ mJ mole}^{-1} \text{K}^{-2}$ . For the Er system we estimate from this plot that the maximal  $\gamma$  value attains  $200 \text{ mJ mole}^{-1} \text{K}^{-2}$ . For all  $R\text{Co}_2$  compounds ( $R = \text{Er}, \text{Ho}, \text{Dy}, \text{Tb}, \text{Gd}$ ) in Fig. 10 the ferromagnetic and paramagnetic Curie temperatures ( $T_C, \Theta_p$ ) were drawn from the review article of Buschow.<sup>33</sup>

For a further discussion we subdivide the extended magnetically disordered range ( $0 < x < 0.45$ ) into two regimes since  $C_m$  behaves significantly different for  $x > 0.2$  and  $x \leq 0.2$ :

(i) The more concentrated range ( $0.2 < x < 0.45$ ) is characterized by pronounced freezing effects in the magnetization and an approximate scaling of  $C_m/x$  versus the reduced temperature  $T/x$ . Such a scaling behavior of  $C_m$  indicates a random freezing of magnetic moments with RKKY interactions.<sup>28</sup> However, a better scaling behavior of  $C_m$  is obtained if we use a  $C_m/(x^{1.7})$ -versus- $T/x$  plot instead of  $C_m/x$  versus  $T/x$ . This deviation from the simple scaling law may be caused by the appearance of the induced Co moment for  $x > 0.2$  observed in the magnetization measurements. As it is also detected in other spin-glass systems<sup>34</sup> the broad maxima of  $C_m$  lie above the sharp peaks of the ac susceptibility and vary almost linearly with the concentration. The magnetic entropy per Ho atom remains constant and attains nearly the theoretical value of  $23.6 \text{ J mole}^{-1} \text{K}^{-1}$  as in the long-range-ordered range (Fig. 7). This is a further strong indication that the induced Co moment can be referred to as itinerant in the sense of the Stoner theory since the magnetic entropy ( $R \ln 2$ ) associated with spin  $\frac{1}{2}$  can neither be detected in this regime nor in the long-range-ordered concentration range  $x \geq 0.5$ .

(ii) In the dilute regime ( $0 < x < 0.2$ ) we find a different scaling behavior of  $C_m$  ( $C_m/x$  versus  $T$ ) and an unusually large enhancement of  $\gamma$  as a function of  $x$  [ $\gamma = 36 \text{ mJ mole}^{-1} \text{K}^{-2}$  and  $160 \text{ mJ mole}^{-1} \text{K}^{-2}$  for  $\text{YCo}_2$  and  $(\text{Ho}_{0.2}\text{Y}_{0.8})\text{Co}_2$ ] together with significant low-temperature upturns of  $C_p/T$ -versus- $T^2$  plots and an increase of the Debye temperatures (see Figs. 4, 5, and 7). Furthermore, the magnetic entropy per Ho,  $S_m/x$ , is drastically reduced. These facts, namely the loss of magnetic entropy and the low-temperature upturns of  $C_p/T$ , cannot simply be attributed to a Schottky peak below 1.5 K since the maxima of the magnetic heat capacity remain almost independent of  $x$  at about 10 K for  $x \leq 0.1$ . In order to explain the low-temperature upturns of  $(C_p - C_n)/T$  in the dilute limit one may assume that a second Schottky anomaly due to magnetic clusters occurs at lower temperatures. However, this is rather unlikely; such an assumption is not valuable to explain the large  $\gamma$  enhancement as a function of  $x$ .

There is no doubt that the transition from the strongly enhanced paramagnetic state to long-range ferrimagnetism proceeds in this system not via a simple clearcut spin-glass and cluster-glass regime. We suppose that additional spin fluctuations and/or Kondo scattering mechanisms contribute to the specific-heat anomalies observed. In this regard it is noteworthy that the pronounced resistivity minima just above  $T_C$  or  $T_f$  appear to be intimately correlated with deep minima of the thermo-

power observed by Gratz *et al.*<sup>15</sup>

From the above comparison of  $(\text{Ho}, \text{Y})\text{Co}_2$  with the other heavy  $(R, \text{Y})\text{Co}_2$  systems, we deduced that the maximal  $\gamma$  and  $x_c$  values vary inversely with the de Gennes factor (see Fig. 10). This may be used as a hint that as the magnetic exchange energy decreases in this series the more unstable appears to be the  $R$  moment in the dilute limit and the larger is the influence of spin fluctuations and probably a Kondo scattering mechanism.

The recent theory proposed by Edwards<sup>35</sup> presumably accounts for the various anomalies observed in the Ho system, as the large  $\gamma$  enhancement, the reduction of the magnetic entropy  $S_m/x$  below  $x=0.2$  together with the pronounced resistivity and thermopower minima. Edwards discussed the breakdown of normal magnetic order in  $R$  metals in terms of the magnetically ordered Anderson lattice: the Anderson lattice undergoes a phase transition from a magnetic to a nonmagnetic ground state as the hybridization of the  $4f$  states with the conduction band is increased. As the magnetic instability is approached sharp but weak  $f$  spectral weight just above the down-spin Fermi level hybridizes strongly with the conduction band and leads to rapidly increasing mass enhancement. This mass enhancement is discussed in terms of magnon energies; the detailed calculation uses a constant magnon energy with a gap of 5 meV. The spin-wave spectrum of  $\text{HoCo}_2$  indeed exhibits a gap of about 4 meV. Thus the transition from a magnetic to a nonmagnetic ground state in  $(\text{Ho}, \text{Y})\text{Co}_2$  may be discussed in terms of this model: the increasing extent of hybridization leading to the mass enhancement may presumably arise from a reduction of the magnon gap as Ho is substituted by Y. Resistivity and thermopower minima are detected for both compounds with a magnetic and a nonmagnetic ground state; the maximal  $\gamma$  enhancement, however, occurs at  $x=0.2$  in the disordered regime, just where Ho is on the verge of inducing the Co moment. This theory can probably account for the reduction of the magnetic entropy per Ho atom for  $x < 0.2$  in terms of a shielding mechanism of the local Ho moment.

The magnetic entropy obtained by integrating  $C_m/T$  is shown for various  $x$  values as a function of temperature in Figs. 11(a) and 11(b). As already mentioned the magnetic entropy per Ho atom attains the theoretical value for  $J=8$  [ $R \ln(2J+1)=23.6 \text{ J mole}^{-1} \text{ K}^{-1}$ ] far beyond the freezing temperature or  $T_C$  and remains roughly independent of  $x$  except for  $x < 0.2$  [see also Fig. 7(a)]. This finding gives evidence for the itinerant nature of the induced Co moment since the magnetic entropy ( $R \ln 2=5.76 \text{ J mole}^{-1} \text{ K}^{-1}$ ) associated with spin  $\frac{1}{2}$  can neither be detected in the magnetically disordered nor in the long-range-ordered concentration range. In contrast to local moments, itinerant moments disappear at  $T_C$  and therefore give rise to a large volume expansion just below  $T_C$  and a vanishing magnetic entropy at  $T_C$ . The latter can be shown easily by integrating  $C_m/T$ , where  $C_m$  is given within the Stoner theory,<sup>36,37</sup>

$$C_m = -\gamma_m T + \beta_m T^3. \quad (6)$$

Both effects—a large volume expansion<sup>17,18</sup> and the van-

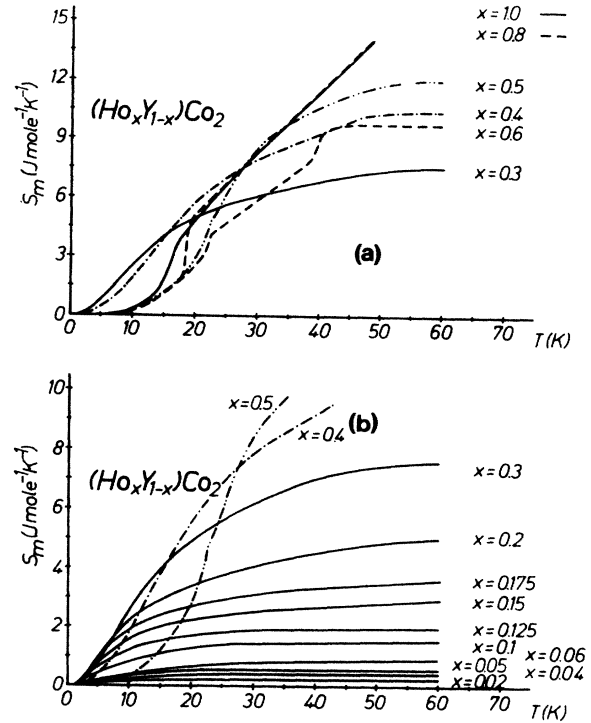


FIG. 11. (a) and (b).  $S_m$  vs  $T$  of  $(\text{Ho}, \text{Y})\text{Co}_2$  for  $0 < x \leq 1$ .

ishing magnetic entropy associated with the Co moment—are observed.

Further evidence for the appearance of an itinerant moment can be derived from a more detailed inspection of the magnetic entropy in Figs. 11(a) and 11(b). Up to  $x=0.2$  the  $S_m(T)$  plots exhibit a negative curvature at low temperatures while positive curvatures occur for  $x > 0.2$ . This change of the curvature can be attributed to the first negative term of  $C_m$  in Eq. (6) and is intimately correlated with the appearance of an itinerant moment. The positive curvature increases with the rising Co moment which attains  $1\mu_B$  and remains constant for  $x > 0.5$ . Therefore we expect for  $x > 0.5$  a constant positive curvature of  $S_m$  since the leading term of the linear negative magnetic heat capacity is the square of the itinerant magnetization, which is indeed observed. This seems to be the first experimental evidence of the negative term of  $C_m$  in the Stoner theory according to Eq. (6).

The enhancement of the Debye temperatures is a further anomaly in the dilute Ho-concentration range. Their determination is not unambiguous but is correlated with the evaluation of the  $\gamma$  values whereby the linear high-temperature limit of the  $(C_p - C_n)/T$ -versus- $T^2$  plots were conservatively used. A comparison with the Tb system shows that Kuentzler and Tari<sup>31</sup> obtained a minimum of  $\Theta_D$  at the critical concentration. However, if we use their unevaluated data of  $(\text{Tb}_{0.05}\text{Y}_{0.95})\text{Co}_2$  to estimate  $\Theta_D$  we obtain fairly high  $\Theta_D$  values at about  $x_c$ , where  $\gamma$  also exhibits a peak. Since spin fluctuations and/or a Kondo scattering can give rise to the  $\gamma$  enhancement we tentatively suppose that spin fluctuations also effect the phonon contribution to the heat capacity.

Mohn, Wagner, and Wohlfarth<sup>38</sup> showed recently that spin fluctuations in itinerant systems can give rise to a positive effective magnetic pressure while the appearance of an itinerant moment in the Stoner theory leads to a negative pressure causing a volume expansion. This effect has also been proposed by Pettifor<sup>39,40</sup> and more recently by Holden, Heine, and Samson.<sup>41</sup> The common feature of these theories is an expression for the magnetic part of the thermal volume expansion which consists of two competing terms with opposite sign.

This model seems to be consistent with the paramagnon model<sup>42</sup> where the low-temperature heat capacity is given by

$$C_p = AT + BT^3 + DT^3 \ln T \quad (7)$$

with  $A = \gamma_0(1 + \lambda_{e-ph} + \lambda_{SF})$ ,  $B = \beta - D \ln T_{SF}$  ( $\lambda_{e-ph}$  is the electron-phonon enhancement and  $T_{SF}$  is the spin-fluctuation temperature). The spin-fluctuation enhancement factor  $\lambda_{SF}$  and the coefficient  $D$  depend upon the extent of the spin fluctuations and both can be reduced by an external magnetic field. This is plausible since a sufficiently large magnetic field causes an energy splitting of opposite spin states which is comparable or larger than the characteristic spin-fluctuation energy ( $kT_{SF}$ ) to flip the spin. Thus a magnetic field stabilizes the fluctuating moments and quenches the spin fluctuations. In this model the spin fluctuations reduce the Debye-lattice contribution  $\beta$ , resulting in a smaller  $B$  value which corresponds to a larger effective Debye temperature. This is consistent with the former model where spin fluctuations also contribute with a linear term in temperature to the specific heat and are discussed in terms of an effective pressure which cause a stiffening of the lattice or an effective  $\Theta_D$  enhancement.

Although the  $T^3 \ln T$  term could not be observed in  $\text{YCo}_2$ —as in many other known spin-fluctuation materials<sup>43</sup>—the application of an external field of 10 T reduces the linear term  $A$  and enhances  $B$  in Eq. (7) by about  $-4\%$  and  $18\%$ , respectively. Ikeda *et al.*<sup>6</sup> derived from these experiments the evidence for the existence of spin fluctuations and their quenching in external fields for  $\text{YCo}_2$ .

In this context one would simply expect that on substituting Y by Ho the growing Ho molecular field reduces the spin fluctuations since this molecular field induces for higher Ho content the itinerant Co moment. However, just the opposite is observed. Both  $\lambda$  and  $\Theta_D$  increase rather drastically. This implies—in terms of the above-mentioned models—that the contributions of the spin fluctuations increase up to  $x=0.2$  where the itinerant moment is started to be induced. By analogy with specific-heat measurements of  $\text{YCo}_2$  in external fields these results appear to be a paradox. However, considering the random freezing of the Ho moments we suppose that the local Ho molecular fields are also randomly oriented and cancel each other and seem therefore to be of minor importance for a quenching of spin fluctuations up to  $x=0.2$ . Presumably the frustrated Ho moments with their randomly oriented molecular fields give rise to the enhancement of spin fluctuations for  $0 < x < 0.2$ . The in-

creasing extent of spin fluctuations derived from  $\gamma$  and  $\Theta_D$  enhancement seem to depend on the stability of the R moment and the extent of the disordered regime: the lower the  $T_C$  of the respective  $\text{RCO}_2$  compound, the higher the critical concentration and the maximal  $\gamma$  value (see Fig. 10).

Although the origin of the increasing contribution of the spin fluctuations up to  $x=0.2$  remains speculative, it may presumably arise from an instability of the Ho moment. We can qualitatively explain the  $\gamma$  and  $\Theta_D$  variation in terms of the above-mentioned models. The increasing extent of spin fluctuations causes a  $\gamma$  enhancement and gives rise to a lattice compression, but the appearance of the induced Co moment at about  $x=0.2$  has a counteracting effect upon both the effective  $\gamma$  and  $\Theta_D$  values: qualitatively we expect that the stiffening of the lattice, which implies an increase of  $\Theta_D$ , is compensated by the volume expansion due to the occurrence of the itinerant Co moment. With the increase of the induced Co moment the spin fluctuations are gradually quenched and  $\gamma$  and  $\Theta_D$  decrease but remain almost constant in the long-range-ordered regime.

## V. CONCLUSION

Significant anomalies in transport phenomena and magnetic properties around the critical concentration for the onset of magnetism make these systems attractive for extensive heat-capacity studies.

The extended magnetically disordered region ( $0 < x < 0.45$ ) can be characterized by a superposition of various effects: (i) the random freezing of the diluted Ho moments, (ii) the occurrence of spin fluctuations, and (iii) the induction of the itinerant Co moment by the Ho molecular field.

The random freezing of the localized Ho moments appears to be the dominant contribution to the heat capacity for  $0.15 < x < 0.45$ . The variation of  $\gamma$  and  $\Theta_D$  can be explained satisfactorily by an increasing extent of spin fluctuations which are progressively quenched for  $x > 0.2$  as the Co moment is stabilized and long-range order is approached for  $x > 0.4$ . However, the detailed question of what origin is the increasing extent of the spin fluctuations remains speculative but may arise from an instability of the Ho moment according to a model presented recently by Edwards.<sup>35</sup> The significant change of entropy curves for rising  $x$  values indicates that starting from  $x \geq 0.2$  an itinerant Co moment is progressively induced. The grand total magnetic entropy per Ho atom remains above  $T_C$  or the freezing temperature  $T_f$  almost independent of  $x$  for  $0.2 < x < 1.0$  and attains only the theoretical value for Ho ( $23.6 \text{ J mole}^{-1} \text{ K}^{-1}$ ). The vanishing magnetic entropy associated with the Co moment above  $T_C$  gives together with magnetic and magnetovolume experiments a further piece of evidence that the Co moment can be referred to as itinerant in the sense of the Stoner theory.

## ACKNOWLEDGMENT

This work was supported by the Austrian Science Foundation (Fonds zur Förderung der wissenschaftlichen Forschung in Österreich) under Project No. 6104.



- <sup>1</sup>R. Lemaire and J. Schweizer, *Phys. Lett.* **21**, 366 (1966).
- <sup>2</sup>F. Givord and J. S. Shah, *C. R. Acad. Sci. Paris, Sec. B* **274**, 923 (1972).
- <sup>3</sup>W. Steiner, E. Gratz, H. Ortbauer, and H. W. Camen, *J. Phys. F* **8**, 1525 (1978).
- <sup>4</sup>R. Lemaire, *Cobalt* **33**, 201 (1966).
- <sup>5</sup>D. Bloch, F. Chaisse, F. Givord, J. Voiron, and E. Burzo, *J. Phys. (Paris)* **32**, C1-659 (1971).
- <sup>6</sup>K. Ikeda, K. A. Gschneidner, Jr., R. J. Stierman, T.-W. E. Tsang, and O. D. McMasters, *Phys. Rev. B* **29**, 5039 (1984).
- <sup>7</sup>M. Cyrot and M. Lavagna, *J. Phys. (Paris)* **40**, 763 (1979).
- <sup>8</sup>E. P. Wohlfarth, *J. Phys. F* **9**, L123 (1979).
- <sup>9</sup>K. Schwarz and P. Mohn, *J. Phys. F* **14**, L129 (1984).
- <sup>10</sup>H. Yamada and M. Shimizu, *J. Phys. F* **15**, L175 (1985).
- <sup>11</sup>R. M. Moon, W. C. Koehler, and J. Farrell, *J. Appl. Phys.* **36**, 978 (1965).
- <sup>12</sup>D. Bloch, D. M. Edwards, M. Shimizu, and J. Voiron, *J. Phys. F* **5**, 1217 (1975).
- <sup>13</sup>N. H. Duc, T. D. Hien, P. E. Brommer, and J. J. M. Franse, *J. Phys. F* (to be published).
- <sup>14</sup>J. Inoue and M. Shimizu, *J. Phys. F* **12**, 1811 (1982).
- <sup>15</sup>E. Gratz, E. Bauer, V. Sechovsky, and J. Chmíst, *J. Magn. Magn. Mater.* **54-57**, 517 (1986).
- <sup>16</sup>S. Hirose and Y. Nakamura, *J. Phys. Soc. Jpn.* **51**, 2819 (1982).
- <sup>17</sup>Y. Muraoka, M. Shiga, and Y. Nakamura, *J. Magn. Magn. Mater.* **31-34**, 121 (1983).
- <sup>18</sup>Y. Muraoka, H. Okuda, M. Shiga, and Y. Nakamura, *J. Phys. Soc. Jpn.* **53**, 331 (1984).
- <sup>19</sup>Y. Berthier, D. Gignoux, R. Kuentzler, and A. Tari, *J. Magn. Magn. Mater.* **54-57**, 479 (1986).
- <sup>20</sup>C. Schmitzer, Ph.D. thesis, Technical University of Vienna, 1985 (unpublished).
- <sup>21</sup>D. Gignoux, F. Givord, and R. Lemaire, *Phys. Rev. B* **12**, 3878 (1975).
- <sup>22</sup>E. Gratz, *Solid State Commun.* **48**, 825 (1983).
- <sup>23</sup>L. J. Sundstroem, in *Handbook on Physics and Chemistry of Rare Earths*, edited by K. A. Gschneidner, L. Eyring (North-Holland, Amsterdam, 1978).
- <sup>24</sup>A. Castets, D. Gignoux, and B. Hennion, *Phys. Rev. B* **25**, 337 (1982).
- <sup>25</sup>F. Keffer, *Handbuch der Physik*, edited by S. Fluegge (Springer, Berlin, 1966), Vol. 18, No. 2, p. 103.
- <sup>26</sup>G. Hilscher, R. Haferl, H. Kirchmayr, M. Mueller, and H. J. Guentherodt, *J. Phys. F* **11**, 2429 (1981).
- <sup>27</sup>J. Balogh and I. Vinze, *Solid State Commun.* **25**, 695 (1978).
- <sup>28</sup>J. Souletie and R. Tournier, *J. Low Temp. Phys.* **1**, 95 (1969).
- <sup>29</sup>T. Sakakibara, T. Goto, K. Yoshimura, M. Shiga, and Y. Nakamura, *Phys. Lett. A* **117**, 243 (1986).
- <sup>30</sup>N. Pillmayr, C. Schmitzer, E. Gratz, G. Hilscher, and V. Sechovsky, *J. Magn. Magn. Mater.* **70**, 162 (1987).
- <sup>31</sup>R. Kuentzler and A. Tari, *J. Magn. Magn. Mater.* **61**, 29 (1986).
- <sup>32</sup>G. Hilscher, N. Pillmayr, V. Sechovsky, and E. Gratz, *J. Magn. Magn. Mater.* **70**, 159 (1987).
- <sup>33</sup>K. H. J. Buschow, *Rep. Prog. Phys.* **40**, 1179 (1977).
- <sup>34</sup>D. L. Martin, *Phys. Rev. B* **20**, 368 (1979).
- <sup>35</sup>D. M. Edwards, *Proceedings of the Fifth International Conference on Valence Fluctuation, Bangalore, India* (Plenum, New York, 1987).
- <sup>36</sup>E. C. Stoner, *Proc. R. Soc. London, Ser. A* **169**, 339 (1939).
- <sup>37</sup>E. P. Wohlfarth, *Physica* **91B**, 305 (1977).
- <sup>38</sup>P. Mohn, D. Wagner, and E. P. Wohlfarth, *J. Phys. F* **17**, L13 (1987).
- <sup>39</sup>D. G. Pettifor, *Phys. Rev. Lett.* **42**, 846 (1979).
- <sup>40</sup>D. G. Pettifor, *J. Magn. Magn. Mater.* **15-18**, 847 (1980).
- <sup>41</sup>A. J. Holden, V. Heine, and J. H. Samson, *J. Phys. F* **14**, 1005 (1984).
- <sup>42</sup>M. T. Beal-Monod and E. Daniel, *Phys. Rev. B* **27**, 4467 (1983).
- <sup>43</sup>K. A. Gschneidner, Jr. and K. Ikeda, *J. Magn. Magn. Mater.* **31-34**, 265 (1983).